Numerical Simulation of Unsteady Rotor Flow Using an Unstructured Overset Mesh Flow Solver

Mun Seung Jung* and Oh Joon Kwon**
Korea Advanced Institute of Science and Technology(KAIST)
335 Gwahangno, Yuseong-gu, Daejeon 305-701, Korea

Abstract

An unstructured overset mesh method has been developed for the simulation of unsteady flow fields around isolated rotors and rotor-fuselage configurations. The flow solver was parallelized for the efficient calculation of complicated flows requiring a large number of cells. A quasi-unsteady mesh adaptation technique was adopted to enhance the spatial accuracy of the solution and to better resolve the rotor wake. The method has been applied to calculate the flow fields around rotor-alone and rotor-fuselage configurations in forward flight. Validations were made by comparing the predicted results with those of measurements. It was demonstrated that the present method is efficient and robust for the prediction of unsteady time-accurate flow fields involving multiple bodies in relative motion.

Key Word : Unstructured overset mesh technique, Helicopter forward flight, Mesh adaptation, Rotor trim

Introduction

The flow fields around helicopter rotors are very complicated, particularly in forward flight, because rotor blades encounter unsteady periodic free stream and are subjected to time-varying wake. Addition of a fuselage underneath the rotor further amplifies the complexity, requiring the solution of unsteady time-accurate three-dimensional flows involving multiple bodies in relative motion.

Several research works have been previously conducted to calculate unsteady flow fields of isolated rotors [1-3] and the complicated flows involving mutual aerodynamic interference between the rotor and the fuselage [4-6]. Recently, structured overset grid methods have been used to study the grid-related effect on the numerical results of hovering rotors [7] and to handle the relative motion between the rotor blades and the fuselage [8-10]. However, structured overset grid methods are not grid-efficient and requirentxcessi[7]y large number of cells to accurately capturenthe vortical wake because of the regularity required in the grid point distribution. On the other hand, unstructured mesh topologies are based on randomly distributed points, and thus are very flexible in generating meshes, particularly for complexmplexmplexmplex, and refining cells ipoi solution-adaptive manner. Application of the unstructured adaptive mesh techniques for solving Euler and Navier-Stokes flows enerating meshes, pplexmplexmplexmplehoverniquesuccessfully accomplisheddaptseveral researchers [11-13]. Recently, aleunstructured sliding mesh method with a quasi-unsteady solution-adaptive technique was also developed for the simulation of unsteady flow fields around helicopter rotors and rotor-fuselage configurations in forward flight [14, 15]. However, the sliding mesh method is not robust when mesh deformation becomes severe due to large blade motion.

* Graduate Research Assistant, Aerospace Engineering
** Professor, Aerospace Engineering
E-mail : ojkwon@kaist.ac.kr Tel : 042-350-3720 Fax : 042-350-3710

In the present study, a parallel unstructured solution-adaptive overset mesh method has been developed for the simulation of unsteady flow fields around helicopter rotors and rotor-fuselage configurations. The relative motion between rotating blades and the fuselage was enabled by overlapping sub-domain meshes containing rotor blades onto the stationary mesh around the fuselage. The spatial accuracy of the solution and the rotor wake capturing were enhanced by adopting a quasi-unsteady solution-adaptive mesh refinement technique. Validations were made by calculating flows around an isolated rotor and a rotor-fuselage configuration in forward flight and comparing the predicted results with measurements.

Numerical Method

Discretization of governing equations

The governing unsteady Euler equations were discretized using a cell-centered finite-volume method in conjunction with Roe's flux-difference splitting. To obtain second-order spatial accuracy, estimation of the state variables at each cell face was achieved by interpolating the solution using a Taylor series expansion in the neighborhood of each cell center for the above expansion was evaluated from the Gauss' theorem by evaluating the surface integral for the closed surface of each tetrahedral cell. The expansion also requires the nodal value of the solution, which was computed from the surrounding cell center data using a second-order accurate pseudo-Laplacian averaging procedure. An implicit time integration algorithm based on a linearized second-order Euler backward difference was used to advance the solution in time. The linear system of equations was solved at each time step using a point Gauss-Seidel method.

On the solid surface of the rotor blades and the fuselage, the flow tangency condition was applied. The density and the pressure on the solid surface were obtained by extrapolating from the interior domain. At the far-field boundary, the pressure was fixed to the freestream value and other flow variables were extrapolated from the interior.

In order to reduce the large computational time, a parallel algorithm based on a domain decomposition strategy was applied. The load balancing between processors was achieved by partitioning the global computational domain into local sub-domains using MeTiS libraries. The Message Passing Interface was used to transfer the flow variables across the sub-domain boundaries. All calculations were made on a PC-based Linux cluster.

Unstructured overset mesh technique

For overset mesh methods, a search procedure is required to identify the cell locations containing the nodes from other mesh blocks. For unstructured meshes, the search is required for all nodes of all mesh blocks because the nodes and cells are randomly distributed. Once the search process is completed for all nodes, the position information of nodes are used for the judgement of active or non-active cells and for the determination of the weighting factors for interpolation. Since this search procedure is very time-consuming, a fast and robust neighbor-to-neighbor search technique was developed based on the property of the linear shape functions by examining the geometric relationship between the beeline connecting the starting position to the target point and the faces of the cells the beeline crosses as shown in Fig. 1(a). The point search under parallel environment was achieved by introducing a new data structure for parallel distributed memory machines as shown in Fig. 1(b).

In the present overset mesh method, the distance-to-wall technique [16] was implemented to distinguish between active and non-active nodes. Determination of active, interpolation, and non-active cells for hole cutting was made based on the number of active nodes assigned to each tetrahedral cell.

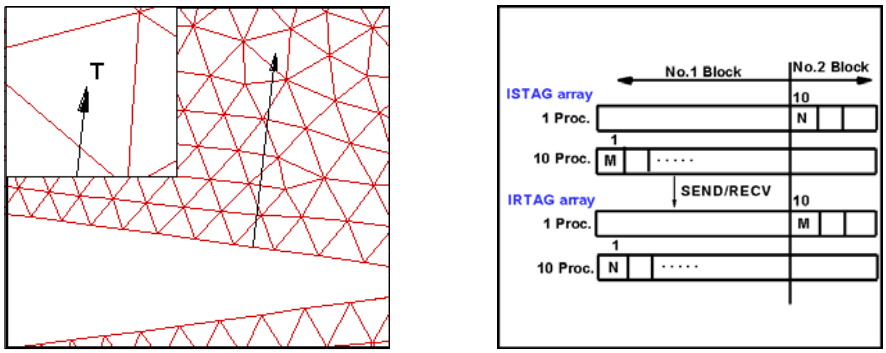

(a) Point search method (b) Data structure for parallelization

Fig. 1. Point search and parallelization

Since transfer of the flow variables between mesh blocks is made through interpolation, the results obtained from overset mesh methods do not satisfy the conservation property. The local solution accuracy degrades more when the characteristic cell size changes drastically from one mesh block to another. In order to reduce this error, the interpolation was made by considering not only the cell containing the interpolation receiver but also the neighbor cells enclosing the cell.

Mesh adaptation

A solution-adaptive mesh adaptation procedure was applied to reduce the numerical dissipation and to enhance the spatial accuracy of the solution. In the present study, a 'quasi-unsteady' mesh adaptation technique [14] was adopted to maintain proper mesh resolution, while avoiding excessive computational time required for the dynamic mesh adaptation applied in a fully unsteady manner.

As the blades rotated, cells having high vorticity were tagged at every time step. Once the rotor completed one period of rotation, the calculation was paused and the mesh adaptation was applied. Then the refined mesh was re-partitioned for load balancing and the calculation resumed. This procedure was repeated several times as necessary. The tagged cells were divided by adding new nodes in the middle of six edges of each tetrahedral cell. Buffer cells were also used to preserve the connectivity between the divided and surrounding cells. The mesh adaptation was performed for each mesh block, independent to other blocks.

In order to reduce the interpolation error, those cells at and near the interpolation boundary between mesh blocks were also refined when the difference in the characteristic cell sizes between neighboring blocks became too large.

Rotor trim

In order to retain the calculated thrust to a desired level and to eliminate the rotor aerodynamic moment, a rotor trim procedure was adopted. The thrust and moment coefficients can be expressed as a function of the collective and cyclic pitch angles. Then the equilibrium state was obtained by adjusting the trim angles iteratively using the Newton-Raphson method [3,14].

Results and Discussion

Rotor-alone configuration

The first validation was made for a lifting AH-1G rotor in forward flight. The rotor was tested and the data have been well documented for comparison [17]. The blades of the teetering rotor have a rectangular planform shape and an aspect ratio of 9.8. The blades are linearly twisted by -10 degrees from root to tip. The flight measurement compared with the present calculation was made at a tip Mach number of 0.65, an advancing ratio of 0.19, and a time-averaged thrust coefficient of 0.00464.

The measured nomial collective pitch angle was six degrees, and the longitudinal and lateral cyclic pitch angles were −5.5 and 1.7 degrees, respectively. The predicted collective and cyclic pitch angles obtained from the converged trim solution were 5.4, −2.9 and 0.86 degrees, respectively.

In order to model the rotating rotor blades, three unstructured mesh blocks were constructed as shown in Fig. 2. The first block covered the overall stationary flow field and the other two for each of the two rotating blades. The stationary main block composed of 98,381 tetrahedral cells and 16,939 nodes. Each rotational mesh block contained 278,418 tetrahedral cells and 51,624 nodes.

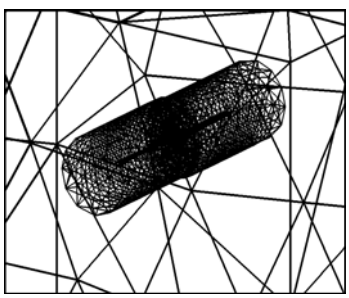

Fig. 2. Computational domain composed of stationary and rotating mesh blocks

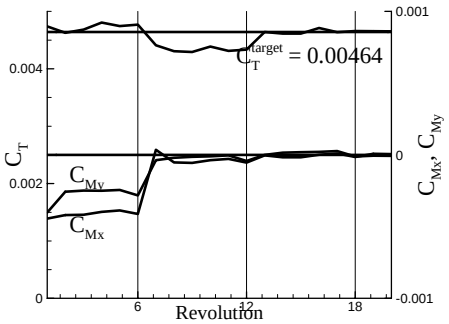

Fig. 3. Trim history of thrust and moment coefficients of the AH-1G rotor in forward flight

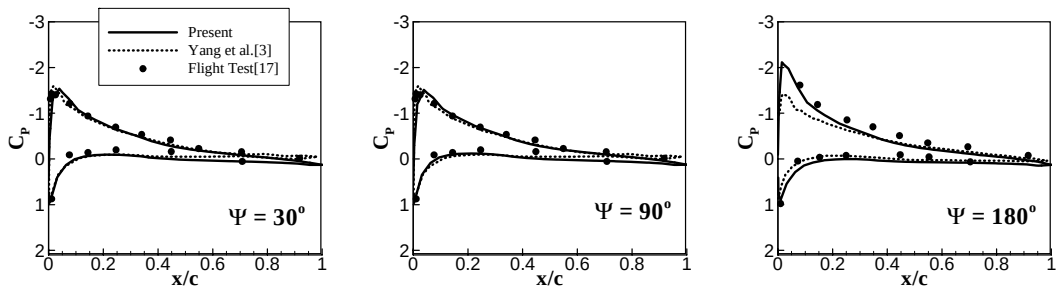

Fig. 4. Chordwise surface pressure distributions of the AH-1G rotor at 60% spanwise section

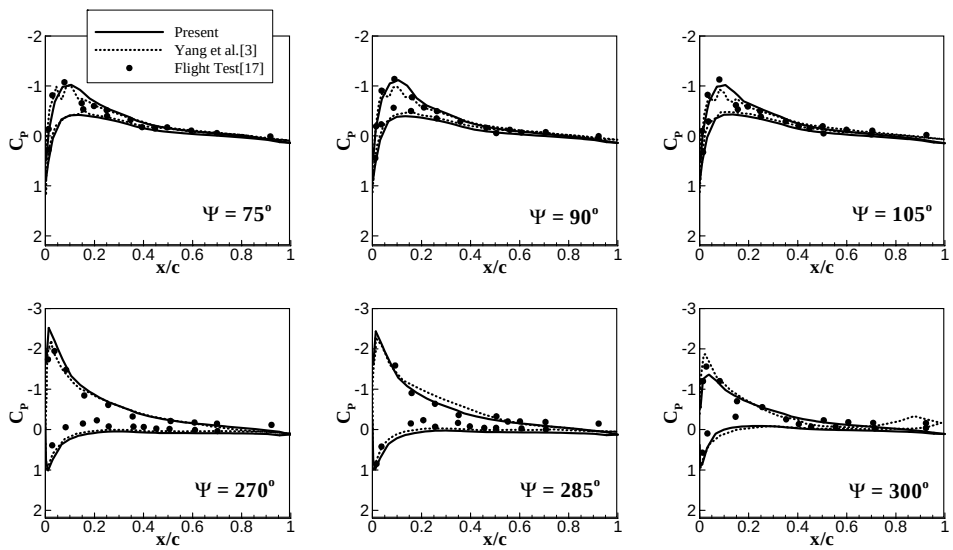

Fig. 5. Chordwise surface pressure distributions of the AH-1G rotor at 91% spanwise section

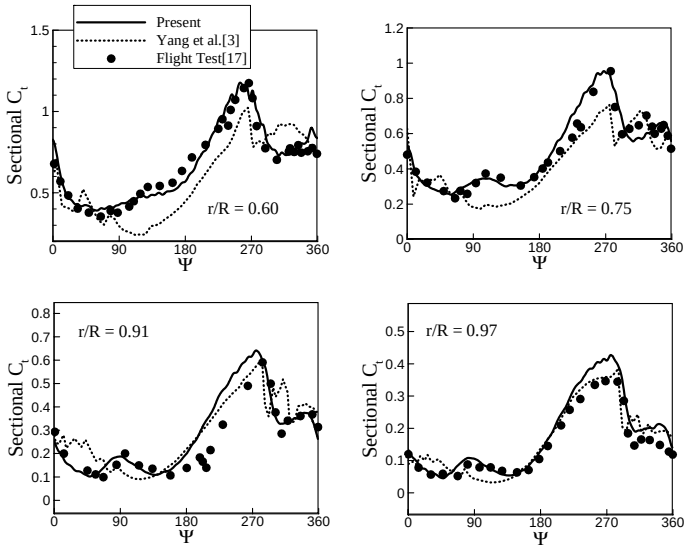

Fig. 6. Sectional thrust variations of the AH-1G rotor blade in forward flight

In Fig. 3, history of the time-averaged thrust and moment coefficients is presented during the rotor trim procedure. It shows that approximately 18 revolutions were required to obtain a converged trim solution. The predicted chordwise surface pressure distributions are compared with the flight test at 60% and 91% spanwise sections in Figs. 4 and 5. The results of a structured mesh method including aeroelastic blade effect [3] are also compared in the figures. It shows that good comparisons were made between the present prediction and the flight test data at all azimuthal positions of the blade for both spanwise stations. The sectional thrust variations at several spanwise locations are compared with the flight test data and the results by a structured grid method [3] in Fig. 6. It shows that the results of the present calculation compare well with the flight test for all spanwise locations. The blade-vortex interaction at the advancing and retreating sides were well captured by the present method.

Rotor-fuselage configuration

The second validation of the present method was made for the rotor-fuselage configuration tested at Georgia Tech [18, 19]. This configuration consisted of a two-bladed teetering rotor and a generic cylinderical fuselage. The blades had an NACA0015 airfoil section and a rectangular planform shape with an aspect ratio of 5.3. The rotor operated at a blade tip Mach number of 0.295 and an advancing ratio of 0.1. The blade collective pitch angle was set to 10 degrees, and the measured thrust coefficient was 0.0091. The rotor shaft had a forward tilt of six degrees.

The initial coarse mesh for this configuration consisted of 499,301 cells in the stationary main block covering the fuselage and 787,261 cells in the rotating blocks for blades. After the second level mesh adaptation, the number of cells increased to 3,032,870 and 2,331,001, respectively. In Fig.7, the computational mesh on the blade and fuselage surfaces and at the fuselage symmetric plane after mesh adaptation is presented. It shows that the cell refinement was mostly made inside the vortical wake around the blades and the fuselage.

In Fig. 8, the time-averaged surface pressure distributions on the fuselage are presented along four circumferential positions. It shows that reasonable comparison was obtained between the present calculation and the experiment for all cases. The present results along the crown line of the fuselage are also comparable with other predicted results based on a momentum source modeling of the rotor [4] and a structured overset grid method [10].

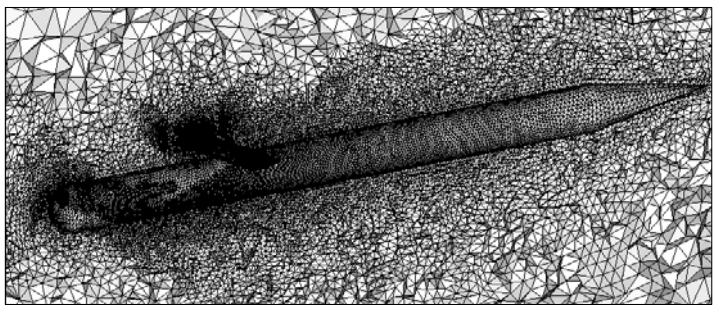

Fig. 7. Computational mesh for the Georgia Tech configuration after mesh adaptation

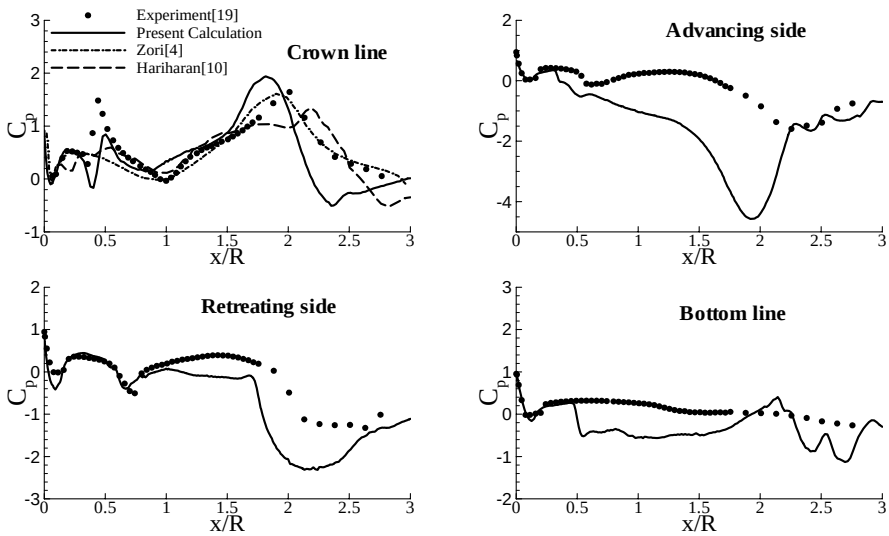

Fig. 8. Time-averaged pressure distribution on the fuselage

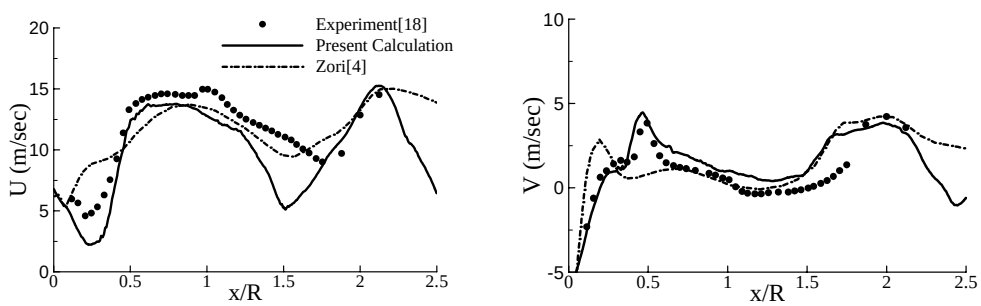

Fig. 9. Time-averaged velocity distribution at 15% chord length above the fuselage

In Fig. 9, the streamwise distributions of the time-averaged downward and streamwise velocity components at 15% chord length above the fuselage are presented. Reasonable agreement was obtained between the present calculation and the experiment for both velocity components. The two peaks and the steep velocity gradient due to the passage of the tip vortex at the front and rear parts of the fuselage were well predicted.

In Fig. 10, the instantaneous pressure distributions along the crown line of the fuselage are presented at four typical blade azimuthal angles. It shows that comparison with the experiment is fair. The effect of blade passage was well predicted at the nose region of the fuselage at zero blade

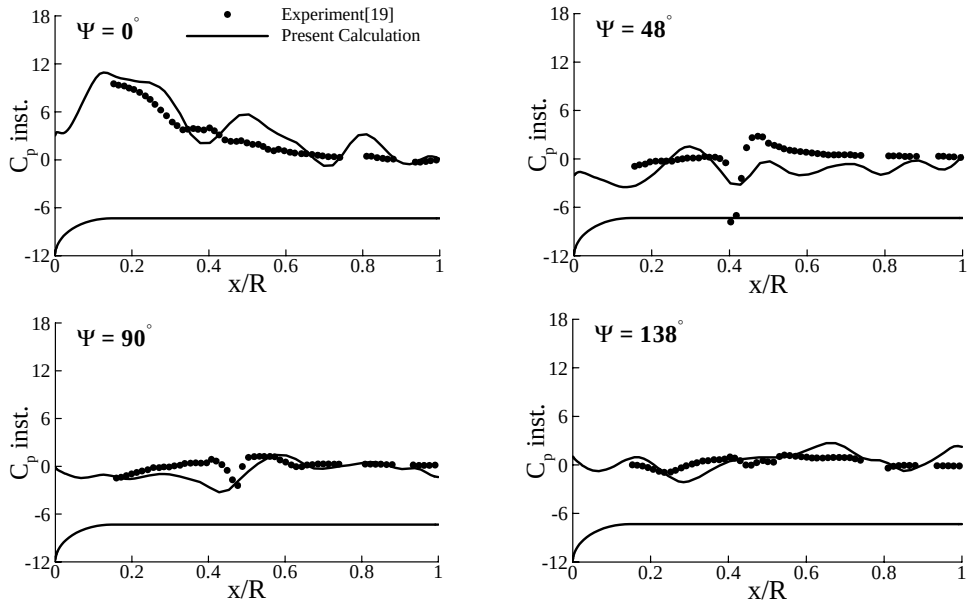

Fig. 10. Instantaneous surface pressure distribution along the crown line of the fuselage

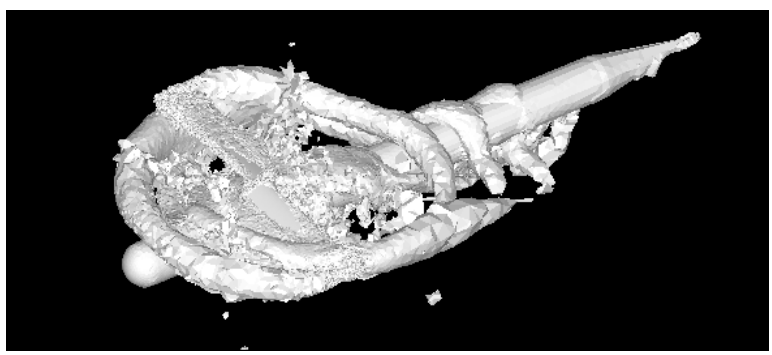

Fig. 11. Instantaneous iso-vorticity surface for the Georgia Tech configuration

azimuth angle. However, the local pressure spike associated with the tip vortex impingement observed by the experiment at the downstream was not properly resolved from the present calculation. This is due to the relatively large mesh resolution to capture the local pressure spike.

In Fig. 11, the perspective view of the instantaneous iso-vorticity surface is presented. Formation of the trailing tip vortex, its migration to the downstream of the rotor, and impingement of the tip vortex on the fuselage can be confirmed in the figure.

Concluding Remarks

A parallel unstructured overset mesh method has been developed for the simulation of unsteady time-accurate flow fields around isolated rotors and rotor-fuselage configurations in forward flight. A quasi-unsteady mesh refinement technique was adopted to enhance the spatial accuracy of the solution. Applications were made to the AH-1G rotor and the Georgia Tech rotor-fuselage configuration. The predicted results compared reasonably well with measurements within the accuracy of the present inviscid calculation. It was demonstrated that the present method is efficient and robust for simulating unsteady rotor flow fields involving multiple bodies in relative motion.

Acknowledgement

This work was supported by Defense Acquisition Program Administration and Agency for Defense Development under the contract UD070041AD.

References

1. Chen, C. L., McCroskey, W. J., and Obayashi, S., "Numerical Solutions of Forward - Flight Rotor Flow Using an Upwind Method", *Journal of Aircraft*, Vol. 28, (6), 1991, pp. 374-380.

2. Bangalore, A., and Sankar, L. N., "Forward-Flight Analysis of slated Rotors Using Navier-Stokes Methods", *Journal of Aircraft*, Vol. 34, (1), 1997, pp. 80-86.

3. Yang, Z., Sankar, L. N., Smith, M., and Bauchau, O., "Recent Improvement to a Hybrid Method for Rotors in Forward Flight", AIAA paper 2000-0260, 2000.

4. Zori, L. A. J., and Rajagopalan, R. G., "Navier-Stokes Calculations of Rotor-Airframe Interaction in Forward Flight", *Journal of the American Helicopter Society*, Vol. 42, (3), 1997, pp. 235-243.

5. Lee, J. K., and Kwon, O. J., "Predicting Aerodynamic Rotor-Fuselage Interactions by Using Unstructured Meshes", *Transaction of the Japan Society for Aeronautical and Space Sciences*, Vol. 44, (146), 2002, pp. 208-216.

6. Boyd, Jr., D. D., Barnwell, R. W., and Gorton, S. A., "A Computational Modelfor Rotor-Fuselage Interactional Aerodynamics", AIAA paper2000-0256,2000.

7. Strawn. R. C., and Djomehri, M. J., "Computational Modelling of Hovering Rotor and Wake Aerodynamics", *Journal of Aircraft*, Vol. 39, (5), 2002, pp. 786-793.

8. Stangl, R., and Wagner, S., "Euler Simulation of a Helicopter Configuration in Forward Flight using a Chimera Technique", American Helicopter Society 52nd Annual Forum, Washington, D. C., 1996.

9. Boniface, J. C., Gullien, Ph., Le pape, M. C., Darracq, D., and Beaumier, Ph., "Development of a Chimera Unsteady Method for the or the or timulation of Rotorcraft Flowfields", AIAA paper 97-0123, 1997.

10. Hariharan, N., and Sankar, L. N., "Unsteady Overset Simulation of Rotor-Airframe Interaction", *Journal of Aircraft*, Vol. 40, (4), 2003, pp. 662-674.

11. Strawn, R. C., and Barth, T. J., "A Finite-Volume Euler Solver for Computing Rotary-Wing Aerodynamics on Unstructured Meshes", *Journal of the American Helicopter Society*, vol. 38, (2), 1993, pp.61-67.

12. Dinder, M., Lemnois, A. Z., Shephard, M. S., and Flaherty, J. E., "An Adaptive Solution Procedure for Rotorcraft Aerodynamics", AIAA paper 98-2417, 1998.

13. Kang, H. J., and Kwon, O. J., "Unstructured Mesh Navier-Stokes Calculations of the Flowfield of a Helicopter in Hover", *Journal of the American Helicopter Society*, vol. 47, (2), 2002, pp. 90-99.

14. Park, Y. M., and Kwon, O. J., "Simulation of Unsteady Rotor Flow Fields Using Unstructured Sliding Meshes", *Journal of the American Helicopter Society*, Vol. 49, (4), 2004, pp. 391-400.

15. Park, Y. M., Nam, H. J., and Kwon, O. J., "Simulation of Unsteady Rotor-Fuselage Interactions Using Unstructured Adaptive Meshes", 59th Annual Forum of the American Helicopter Society, Phoenix, Arizona, May, 2003.

16. Nakahashi, K., Togashi, F., and Sharov, D., "Intergrid-Boundary Definition Method for Overset Unstructured Grid Approach", *AIAA Journal*, Vol. 38, No. 11, 2000, pp. 2077-2084.

17. Cross, J. F., and Tu, W., "Tabulation of Data from the Tip Aerodynamics and Acoustic Test", NASA TM102280, Nov. 1990.

18. Liou, S. G., Komerath, N. M., and McMahon, H. M., "Velocity Measurements of Airframe Effects on a Rotor in Low-Speed Forward Flight", *Journal of Aircraft*, Vol. 26, (4), 1989, pp. 340-348.

19. Brand, A. G., McMahon, H. M., and Liou, S. G., "Surface Pressure Measurements on a Body Subject to Vortex Wake Interaction", *AIAA Journal*, Vol. 27, (5), 1989, pp. 569-574.